


Transferable ionic parameters for first-principles Poisson-Boltzmann solvation calculations: Neutral solutes in aqueous monovalent salt solutions

Cite as: J. Chem. Phys. **146**, 134103 (2017); <https://doi.org/10.1063/1.4978850>

Submitted: 23 December 2016 • Accepted: 02 March 2017 • Published Online: 03 April 2017

Stefan Ringe,  Harald Oberhofer and  Karsten Reuter

COLLECTIONS

 This paper was selected as Featured



View Online



Export Citation



CrossMark

ARTICLES YOU MAY BE INTERESTED IN

[Revised self-consistent continuum solvation in electronic-structure calculations](#)

The Journal of Chemical Physics **136**, 064102 (2012); <https://doi.org/10.1063/1.3676407>

[Generalized molecular solvation in non-aqueous solutions by a single parameter implicit solvation scheme](#)

The Journal of Chemical Physics **150**, 041710 (2019); <https://doi.org/10.1063/1.5050938>

[Grand-canonical approach to density functional theory of electrocatalytic systems: Thermodynamics of solid-liquid interfaces at constant ion and electrode potentials](#)

The Journal of Chemical Physics **150**, 041706 (2019); <https://doi.org/10.1063/1.5047829>

The Journal of Chemical Physics **Special Topics** Open for Submissions [Learn More](#)



Transferable ionic parameters for first-principles Poisson-Boltzmann solvation calculations: Neutral solutes in aqueous monovalent salt solutions

Stefan Ringe,^{a)} Harald Oberhofer, and Karsten Reuter

Chair for Theoretical Chemistry and Catalysis Research Center, Technische Universität München, Lichtenbergstr. 4, D-85747 Garching, Germany

(Received 23 December 2016; accepted 2 March 2017; published online 3 April 2017)

Implicit solvation calculations based on a Stern-layer corrected size-modified Poisson-Boltzmann (SMPB) model are an effective approach to capture electrolytic effects in first-principles electronic structure calculations. For a given salt solution, they require a range of ion-specific parameters, which describe the size of the dissolved ions as well as thickness and shape of the Stern layer. Out of this defined parameter space, we show that the Stern layer thickness expressed in terms of the solute's electron density and the resulting ionic cavity volume completely determine ion effects on the stability of neutral solutes. Using the efficient SMPB functionality of the full-potential density-functional theory package FHI-aims, we derive optimized such Stern layer parameters for neutral solutes in various aqueous monovalent electrolytes. The parametrization protocol relies on fitting to reference Setschenow coefficients that describe solvation free energy changes with ionic strength at low to medium concentrations. The availability of such data for NaCl solutions yields a highly predictive SMPB model that allows to recover the measured Setschenow coefficients with an accuracy that is comparable to prevalent quantitative regression models. Correspondingly derived SMPB parameters for other salts suffer from a much scarcer experimental data base but lead to Stern layer properties that follow a physically reasonable trend with ionic hydration numbers. *Published by AIP Publishing.* [<http://dx.doi.org/10.1063/1.4978850>]

I. INTRODUCTION

The explicit account of solvation environments in first-principles electronic structure calculations remains a huge computational challenge. Simulating a large enough number of solvent molecules and performing a sufficient sampling to achieve converged thermodynamic properties are still largely intractable, even for numerically most efficient approaches like density-functional theory (DFT) in combination with low-rung exchange-correlation functionals. This holds in particular for electrolytic solutions, where the generally low concentrations of dissolved ions would require even larger simulation cells and more extensive sampling. In this situation, implicit solvation methods enjoy a long-standing popularity.¹ In such embedding techniques, solvation effects on the solute are modeled in an average way, for instance, by describing the solvent as a simple dielectric continuum.^{1–6} To access electrolytic environments, these techniques are combined with distribution models for the dissolved ions.^{7–10} Most commonly the ions are thereby considered as continuous charge densities that adapt to the mean-field electrostatic potential built up by all system components (solute and ions embedded into the solvent continuum).

Poisson-Boltzmann (PB, or Debye-Hückel/Gouy-Chapman) theory^{11–14} is a corresponding ansatz that has experienced a particularly long history of success.^{15–26} Due to

efficient implementations in DFT^{7–10,27–30} or force field^{31–35} program packages, it has become a wide-spread tool for modeling chemical processes in electrolytes. In its original formulation, PB theory only considers point-like ions. This has often proven insufficient to describe ion-specific effects, for instance, for systems with high electrostatic potentials, for which point-like ions would accumulate to unphysically high local ion densities.^{32,36–44} This includes highly charged solutes, enzyme active sites,^{33,45} or charged surfaces like Langmuir monolayers.³⁶ Two most prominent avenues to improve on this limitation of standard PB theory are the size-modified PB (MPB) approach and the coupling with a finite Stern layer (PB+Stern layer = SPB theory or Gouy-Chapman-Stern model), cf. Fig. 1. MPB theory accounts for solvated ion-ion short-range repulsion by introducing finite ion sizes via a statistical lattice model in which the lattice cells are only allowed to be occupied by one ion at a time.^{32,36,37,40,41,43,44} This creates an upper bound for local ionic charge accretion and thereby avoids an overshooting of ion concentrations, e.g., close to high electrostatic potentials. The Stern layer concept⁴⁶ accounts for the existence of a finite solute-solvent layer formed around the solute by strongly or weakly bound solvent molecules.^{47–49} In SPB theory this is simply achieved by introducing an ion-free (ion-exclusion) region between the solvation cavity and the diffusive ionic solution. As illustrated in Fig. 1, this ion-exclusion Stern layer may thereby partly arise from the solvation shells around the ions, which also prevent the latter from further approaching the solute.

^{a)}Electronic mail: stefan.ringe@tum.de

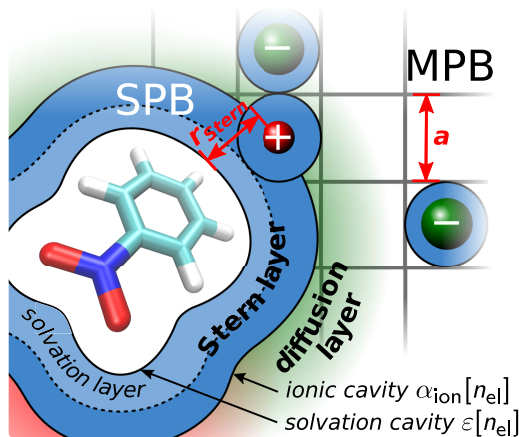


FIG. 1. Schematic representation of an electrolytic environment around a molecular solute, illustrating two prominent modifications of standard Poisson-Boltzmann (PB) theory: A solvent Stern layer of thickness r^{Stern} separates the solute from the diffusive ions in the SPB approach, while MPB theory accounts for more or less rigid solvation shells around the ions by describing them with a finite size a . As apparent from the drawing, the Stern layer can receive contributions from both the solute's solvation layer and the solvation shells around the ions leading to correlation between the corresponding model parameters.

Even though these PB-derived methods have been applied extensively in chemistry,⁵⁰ in particular in (electro-) catalysis,^{51–53} electrochemistry,^{54–56} electrokinetics,^{57,58} and biology,^{15,16,24,26,32,34,59–62} it is often not clear which of the two modifications is really required to achieve an accurate modeling of ion-specific effects. This has led to the pragmatic combination of both strands into MPB plus Stern layer (SMPB) models.^{7,8,29,32,44,63} As is the characteristic for coarse-grained approaches, all three theories (MPB, SPB, and SMPB) depend on a number of effective parameters, describing the ionic size or properties of the Stern layer as its thickness or shape. These parameters can sensitively affect the outcome of corresponding solvation calculations^{7,32,33,63} and need to be carefully determined, for instance, by fitting to the experimental data. Particularly valuable, especially for calculations treating the solute on a first-principles level are thereby transferable parameter sets that can be applied to predict properties for a wide range of solutes and salts.

In this work, we present a corresponding parametrization approach for neutral solutes in aqueous monovalent salt solutions. The protocol relies on fitting to experimentally available Setschenow coefficients, which measure the change of solvation free energy with ionic strength of the electrolyte.^{64,65} After assessing a meaningful parameter space, we first focus on NaCl solutions for which the most experimental data are available. Intriguingly, the thus optimized SMPB parameters describe the measured Setschenow coefficients with an accuracy that is *en par* to prevalent quantitative structure-property relationship (QSPR) regression models. For other salts, SMPB parameters are established correspondingly. In view of the scarcity of experimental reference data, their transferability is less certain though. Encouragingly, we can nevertheless show that the thus defined Stern layer thicknesses yield a reasonable scaling with the number of strongly bound water molecules around the ions (*hydration numbers*) as one would expect from Fig. 1. As such, this scaling can even be used

to derive SMPB parameters for salts not explicitly covered in this work.

II. METHODS

A. Size-modified PB solver including a Stern layer correction

In this paper, we utilize the function-space based SMPB solver⁷ as implemented in the all-electron DFT code FHI-aims.^{66,67} In the following, we only briefly summarize the most important points of this implementation and refer to the original publication for further details and original references.⁷ Unless noted differently, atomic units are used throughout, as is the sign convention commonly employed in DFT, where electronic charge densities have a positive sign. The combined SMPB-DFT method self-consistently minimizes a free energy functional via the common SCF solver with respect to the electron density n_{el} and via a function-space-based combined Newton-multipole expansion relaxation method (Newton-MERM) with respect to the electrostatic potential v . The latter minimization yields the MPB equation

$$\nabla \cdot [\varepsilon[n_{\text{el}}(\mathbf{r})]\nabla v(\mathbf{r})] = -4\pi n_{\text{sol}}(\mathbf{r}) - 4\pi n_{\text{ion}}^{\text{PB}}(\mathbf{r}), \quad (1)$$

with the solute charge density $n_{\text{sol}} = n_{\text{el}} + n_{\text{nuc}}$ (including the nuclei charge density n_{nuc}) and the ionic charge density (for a $z:z$ charged electrolyte)

$$n_{\text{ion}}^{\text{PB}}(\mathbf{r}) = z [c_{+}^{\text{s}}(\mathbf{r}) - c_{-}^{\text{s}}(\mathbf{r})]. \quad (2)$$

Here $c_{+}^{\text{s}}(\mathbf{r})$ and $c_{-}^{\text{s}}(\mathbf{r})$ are the spatially-dependent concentrations of the dissolved cations and anions, respectively. The dielectric function $\varepsilon[n_{\text{el}}(\mathbf{r})]$ entering Eq. (1) is parametrized as a function of the electron density and adopts the value of 1 inside the solvation cavity and $\varepsilon^{\text{s,bulk}}$ outside

$$\varepsilon_{n_{\text{min}}, n_{\text{max}}}[n_{\text{el}}] = \begin{cases} 1 & n_{\text{el}} > n_{\text{max}}, \\ e^{t(\ln(n_{\text{el}}))} & n_{\text{min}} < n_{\text{el}} < n_{\text{max}}, \\ \varepsilon^{\text{s,bulk}} & n_{\text{el}} < n_{\text{min}}, \end{cases} \quad (3)$$

with

$$t(\ln(n_{\text{el}})) = \frac{\ln(\varepsilon^{\text{s,bulk}})}{2\pi} \left[2\pi \frac{\ln(n_{\text{max}}) - \ln(n_{\text{el}})}{\ln(n_{\text{max}}) - \ln(n_{\text{min}})} - \sin \left(2\pi \frac{\ln(n_{\text{max}}) - \ln(n_{\text{el}})}{\ln(n_{\text{max}}) - \ln(n_{\text{min}})} \right) \right], \quad (4)$$

where $\{n_{\text{min}}, n_{\text{max}}\}$ define the dielectric transition and $\varepsilon^{\text{s,bulk}}$ is the static dielectric permittivity of the solvent. Here and henceforth, the explicit dependence on \mathbf{r} is dropped for greater legibility.

The ionic concentrations in the SMPB model are given by

$$c_{\pm}^{\text{s}} = c^{\text{s,bulk}} \alpha_{\text{ion}}^{\pm}[n_{\text{el}}] \times \frac{\exp(\mp z v / (k_{\text{B}} T))}{1 - \phi_0 + \frac{1}{2} \phi_0 \left[\alpha_{\text{ion}}^{+}[n_{\text{el}}] e^{-z v / (k_{\text{B}} T)} + \alpha_{\text{ion}}^{-}[n_{\text{el}}] e^{z v / (k_{\text{B}} T)} \right]}, \quad (5)$$

with $c^{\text{s,bulk}}$ denoting the bulk concentration of the salt, k_{B} the Boltzmann constant, T the temperature, $\phi_0 = 2a^3 c^{\text{s,bulk}}$ the volume fraction of the bulk electrolyte occupied by ions, and a the finite ion size or lattice cell length in the MPB lattice model.³⁶ The smooth ion-exclusion functions $\alpha_{\text{ion}}^{\pm}[n_{\text{el}}]$ are also

parametrized as a function of the electron density and in contrast to our previous paper, we here allow for two independent functions for cations (negative sign) and anions (positive sign), respectively, to increase the flexibility of our model

$$\alpha_{\text{ion}, n_{\text{min}}^{\alpha, \pm}, n_{\text{max}}^{\alpha, \pm}}^{\pm} [n_{\text{el}}] = \begin{cases} 0, & n_{\text{el}} > n_{\text{max}}^{\alpha, \pm}, \\ \frac{1}{\varepsilon^{\text{s, bulk}} - 1} (e^{t(\ln(n_{\text{el}}))} - 1), & n_{\text{min}}^{\alpha, \pm} < n_{\text{el}} < n_{\text{max}}^{\alpha, \pm}, \\ 1, & n_{\text{el}} < n_{\text{min}}^{\alpha, \pm}, \end{cases} \quad (6)$$

where the function t is now evaluated with the isodensity values $\{n_{\text{min}}^{\alpha, \pm}, n_{\text{max}}^{\alpha, \pm}\}$ which define the concentration transition for cations and anions.

B. Model parameters

This methodology gives rise to a range of effective parameters that have to be determined. For the non-ionic parameters, we use the solvation model from Andreussi *et al.*, which was shown to yield accurate solvation energies for neutral molecules in water.⁵ In this model, the parameters $n_{\text{min}} = 0.0001$ and $n_{\text{max}} = 0.005$ define the electron density region in which the dielectric function switches from its bulk value $\varepsilon^{\text{s, bulk}} = 78.36$ to 1, cf. Eq. (3). Additionally, parameters $\alpha + \gamma = 50$ dyn/cm and $\beta = -0.35$ GPa are utilized to model non-electrostatic interactions between solute and water.^{5,7} We note that compared to our original publication,⁷ we now implemented the latter interactions in FHI-aims similar to Andreussi *et al.*, i.e., also in a self-consistent way by adding the functional derivative of the free energy term with respect to the electron density to the Kohn-Sham Hamiltonian. Although we found this to be of minor importance for the evaluation of solvation energies,⁷ it gives us a complete self-contained physical model.

This leaves the ionic parameters, the determination of which is the topic of the present paper. The size parameter a from the original MPB method models the size of the lattice cells and therefore the steric crowding of ions.³⁶ The additional Stern layer in the SMPB approach is defined through the exclusion functions $\alpha_{\text{ion}}^{\pm}$ for cations and anions. For these ion exclusion functions, Eq. (6) employs the same functional form for the transition at the cavity boundary as the dielectric function, only that the $\alpha_{\text{ion}}^{\pm}$ become 1 in the bulk electrolyte and vanish inside the ionic cavity, i.e., inside the combined Stern layer and solvation cavity. The electron density cutoffs $n_{\text{min/max}}^{\alpha, \pm}$ for the ion exclusion functions are then directly related to the cutoffs from the dielectric function transition $n_{\text{min/max}}$,

$$n_{\text{min/max}}^{\alpha, \pm} = \exp\left(\alpha_{\text{min/max}}^{\pm} \pm (a_{\text{max}}^{\pm} - a_{\text{min}}^{\pm}) \frac{1 - \xi_{\alpha_{\text{ion}}^{\pm}}}{2}\right), \quad (7)$$

with

$$a_{\text{min/max}}^{\pm} = \ln(n_{\text{min/max}}) + (\ln(n_{\text{min}}) - \ln(n_{\text{max}})) d_{\alpha_{\text{ion}}^{\pm}}^{\pm}. \quad (8)$$

$d_{\alpha_{\text{ion}}^{\pm}}^{\pm} (d_{\alpha_{\text{ion}}^{\mp}}^{\mp}) > 0$ hereby yields a finite cation(anion)-free Stern layer around the solvation cavity and a lowering (raise) of $\xi_{\alpha_{\text{ion}}^{\pm}}$ to a sharpening (smoothing) of the Stern layer transition for the corresponding ion type.

Apart from specific systems, such as, for instance, highly charged solutes in contact with the ions of low complexing ability,⁶⁸ one can generally expect the existence of some kind

of Stern layer.^{7,48,49,54,69,70} This layer can be considered as a shift of the solute-ion radial distribution functions (RDFs) further outward than the solute-solvent RDF, cf. Fig. 1. While finite ion sizes as included in the MPB model can also prevent over-crowding of ions by the introduction of steric ion-ion repulsions, only the explicit inclusion of solute-ion interaction potentials can provide these observed different offsets of the solute-ion RDF. While sometimes disputed,^{44,62} the inclusion of a volume-based (MPB) ion exclusion does therefore not suppress the need for a distance-based (SPB) ion exclusion (Stern layer correction) since both modifications address different physical short-comings of PB theory. Similarly, there are indications that the inclusion of solvated ion-ion interactions through MPB does give additional improvement that can not be reached by a Stern layer alone, in particular for large ions or close to high electrostatic potentials due to high local ion densities.^{7,33,44,62,70} While this generally motivates the use of the combined SMPB model, it is also clear that both corrections, MPB and SPB, are partly correlated, cf. Fig. 1. Parameter optimization disregarding one or the other correction may therefore lead to physically unrealistic parameters,^{32,63} while simultaneous unconstrained optimization may lead to overfitted models with little transferability (*vide infra*).

From their physical origin, the ion size parameter a and the Stern layer thickness r_{Stern} should depend on ionic properties like hydrated radii or hydration numbers of the ions.^{47,71} For the size parameter a , exclusive correlations with hydrated ion sizes have thereby a reasonable legitimation.⁶³ In contrast, the Stern layer thickness is an effective parameter that results from the interactions of multiple different species such as attractive^{60,72–76} and repulsive solute-ion, solute-solvent, or ion-ion interactions. It will therefore also depend strongly on properties of the solute. This makes it unlikely that parametrization strategies for r_{Stern} that exclusively draw on solute-independent ion sizes^{31,33,35,44,68,73} will lead to much transferability. More general procedures that also consider an explicit dependence on the solute have instead hitherto only met limited success,^{63,77,78} as fitting Stern layer parameters to chemically most diverse solutes is a difficult to impossible task.⁶⁸ In the SMPB-DFT approach, this problem can be efficiently addressed by modeling the Stern layer thickness as a function of both ionic properties and the solute's electron density. With a single choice of the parameters $d_{\alpha_{\text{ion}}^{\pm}}$ and $\xi_{\alpha_{\text{ion}}^{\pm}}$ for a particular salt solution, r_{Stern} will then automatically adapt to the size of the solute as measured by the extent of the electron density.

C. Database of Setschenow coefficients

The determination of transferable SMPB parameters requires accurate experimental data covering a diverse range of solute molecules, salts, and ionic strengths. Among experimentally accessible observables, solvation free energy changes with ionic strengths,

$$\Delta\Delta G_{\text{ion}}(c^{\text{s, bulk}}) = \Delta G_{\text{sol}}(c^{\text{s, bulk}}) - \Delta G_{\text{sol}}(c^{\text{s, bulk}} = 0) \quad (9)$$

(with $\Delta G_{\text{sol}}(c^{\text{s, bulk}})$ the solvation free energy at concentration $c^{\text{s, bulk}}$), are hereby particularly appealing. While for electrolytic solutes, these changes scale according to Debye-Hückel theory with the square root of the ionic concentration,⁷

neutral solutes show a linear regime

$$\Delta\Delta G_{\text{ion}} = k_s \frac{k_B T}{\log_{10}(e)} c^{\text{s,bulk}} \quad (\text{linear}), \quad (10)$$

where k_s is the so-called Setschenow coefficient depending on the solute and salt of choice.^{64,65} For most systems, k_s is positive indicating a reduction of the solubility of the dissolved molecules called *salting-out* effect.

In contrast to incidences observed for more complex salts,⁷⁹ the linear Setschenow regime typically holds up to salt molarities as high as 2M–5M for alkali halide salt solutions.^{65,80–82} Over the years, different collections of molecular Setschenow coefficients in aqueous NaCl solutions have appeared.^{80,83–86} They often contain data from early experimental measurements though, which are likely affected by experimental uncertainties. Setschenow coefficients obtained from fitting entirely to experimental measurements at low ion concentrations are for instance by now known to be prone to high systematic errors which can easily yield uncertainties up to 0.04 l/mol.^{80,85} Likewise, k_s for strongly polar molecules obtained from solubility measurements are masked by solute-solute self-interaction energy changes.⁶⁵ From about 150 experimentally measured molecular Setschenow coefficients in literature,^{49,65,80,83–86} we have therefore built up a database with 95 entries (database **I**^{49,65,84–86}) that is explicitly listed in the [supplementary material](#) (cf. Table S1). The selection was based on highest apparent experimental accuracy but also to arrive at a balanced and broad range of different organic functionalities and physical properties (cf. dipole, polarity, and isotropic static dipole polarizability distributions in the [supplementary material](#), Fig. S1) in the database. This database was exclusively used in the fitting of the SMPB parameters described below. In addition we collected a second validation database (database **I_{val}**⁸⁶) containing 33 Setschenow coefficients of mainly apolar aromatic molecules, cf. Table II and Fig. S1 in the [supplementary material](#), which we used to test the transferability of the determined parameters.

Unfortunately, experimental Setschenow coefficients for salts other than NaCl are very scarce. This does generally not allow to discard data to arrive at balanced sets of different organic functionalities. Nevertheless applying a similar quality selection as for NaCl, we collected a database **II** for various alkali halides as well as NaNO₃ and NH₄Cl salt solutions that in total contains 195 entries.^{65,79,84,87–103} The individual number of molecular reference values for each salt is listed in Table II below, while the whole database is explicitly listed in the [supplementary material](#).

D. Computational setup

All implicit-solvation DFT calculations have been performed with the SMPB functionality of the program package FHI-aims.^{7,66} The exchange-correlation functional due to Perdew, Burke, and Ernzerhof (PBE) has been used throughout.¹⁰⁴ This functional was also used in the optimization of the non-ionic solvation parameters by Andreussi *et al.*⁵ As detailed in the original implementation publication,⁷ use of the default “tight” accuracy settings and the tier2 numeric atomic orbital basis set in FHI-aims yields values of $\Delta\Delta G_{\text{ion}}$ that are numerically converged to 0.01 kcal/mol.

All solute molecule geometries were first relaxed in vacuum until residual forces fell below 0.23 kcal/(mol/Å). These geometries were then taken as a starting point for a subsequent optimization in implicit water using the newly implemented force functionality of the SMPB solver in FHI-aims. Test calculations showed only negligible further geometry changes when reoptimizing these relaxed geometries at finite ionic strength. The experimental Setschenow coefficients in the databases were measured at room temperature. Consistently, we therefore also employed $T = 298.14$ K as ionic temperature in the SMPB model. However, we note that for many neutral solutes, k_s does not show a strong temperature dependence, typically a few percent for variations of ± 20 K.^{105,106}

III. RESULTS

As a first step in the generation of transferable SMPB parameters for first-principles implicit solvation calculations, we here consider the case of neutral solutes in aqueous monovalent salt solutions. In contrast to higher-valent ions where ion correlations are known to play a larger role,¹⁰⁷ SMPB theory is generally expected to perform quite well for this class of salt solutions. Compared to other salts and charged solutes, the parametrization is furthermore simplified by the much higher availability of experimental data, in particular Setschenow coefficients, as well as by the fact that for many neutral solutes, the linear Setschenow regime holds up to medium concentrations of 3–4M.^{65,79–82}

In its full generality, the SMPB model described in Section II A contains five ionic parameters ($a, d_{\alpha_{\text{ion}}}^+, d_{\alpha_{\text{ion}}}^-, \xi_{\alpha_{\text{ion}}}^+, \xi_{\alpha_{\text{ion}}}^-$) that need to be optimized. This already assumes a single ion size a for both cations and anions, and extensions would have to be implemented for the application to the salts with very different anion and cation sizes.³² As discussed in Section II B above, correlations between these ionic parameters are to be expected. An unconstrained optimization by simultaneous fitting to experimental Setschenow coefficients is therefore likely to get trapped in local minima and thereby lead to overfitted models of low predictive quality. In the following, we thus first concentrate on NaCl solutions, for which we can draw on a large experimental database and assess a meaningful parameter space in Section III A. On this basis, we then obtain optimized NaCl SMPB parameters in Section III B and discuss their transferability and reliability. Finally, we determine SMPB parameters also for the other electrolytes in Section III C and use their scaling with ionic hydration numbers to argue in favor of their transferability, despite the scarcity of the reference data that can be used for the optimization.

A. Assessment of SMPB parameter space

We begin assessing a meaningful ionic parameter space for neutral solutes by deriving an approximate analytical expression for $\Delta\Delta G_{\text{ion}}$. This derivation rests on the realization that neutral molecular solutes do not exhibit strong electrostatic fields and will therefore not lead to strong ionic accumulation. This would suggest to approximately consider the electron density of the solute n_{el} and the electrostatic potential v as

unaffected by a finite ionic strength. Starting from the general minimal SMPB free energy expression, Eq. (18) in Ref. 7, this leads to the following approximate expression for the solvation free energy change:

$$\Delta\Delta G_{\text{ion}} \approx -\frac{k_{\text{B}}T}{a^3} \int d\mathbf{r} \ln \left(1 + \phi_0 \left[\alpha_{\text{ion}} \cosh \left(\frac{v}{k_{\text{B}}T} \right) - 1 \right] \right). \quad (11)$$

Here, this expression is given for simplicity for equal ion-exclusion functions $\alpha_{\text{ion}}^{\pm}[n_{\text{el}}] = \alpha_{\text{ion}}[n_{\text{el}}]$ for cations and anions and the full derivation is provided in the [supplementary material](#). Taylor expanding the cosh-term to first order allows to further simplify Eq. (11) to

$$k_{\text{s}} \approx -\frac{\log_{10}(e)}{c^{\text{s,bulk}} a^3} \int d\mathbf{r} \ln(1 + \phi_0(\alpha_{\text{ion}} - 1)), \quad (12)$$

where the expression is given here directly in terms of the Setschenow coefficient as defined by Eq. (10).

This derived equation reveals that in the general case of $a \neq 0$, the Setschenow coefficient is not constant but varies with the ionic concentration. Only the limit $a \rightarrow 0$ allows to recover a linear Setschenow regime as observed experimentally (cf. derivation in the [supplementary material](#))

$$k_{\text{s}}(a \rightarrow 0) \approx 2 \log_{10}(e) V_{\text{ion,cav}}, \quad (13)$$

where $V_{\text{ion,cav}} = \int d\mathbf{r} (1 - \alpha_{\text{ion}})$ is the volume of the ionic cavity as determined by the DFT electron density of the solute in ion-free implicit water and the chosen Stern layer parameters. The generalized form considering different cationic and anionic cavity volumes, $V_{\text{ion,cav}}^{+}$ and $V_{\text{ion,cav}}^{-}$, respectively, can be derived analogously and reads

$$k_{\text{s}}(a \rightarrow 0) \approx \log_{10}(e) (V_{\text{ion,cav}}^{+} + V_{\text{ion,cav}}^{-}). \quad (14)$$

In this limit $a \rightarrow 0$, the Setschenow coefficient is thus uniquely given by the ionic cavity volume. This is consistent with the known correlation of Setschenow coefficients with the solute molecular volume.^{84–86} It also agrees with the current understanding that the dominant contribution for the *salting-out* effect of neutral molecules is a change of the cohesive energy of the aqueous solution by the presence of the ions and the concomitant higher ionic cavity creation costs.⁴⁹

Fig. 2 compares the approximate expressions for the Setschenow coefficient with numerical results obtained from full SMPB-DFT calculations for both a highly polar (cytosine) and an apolar (isopropylbenzene) molecule. Deferring the analysis of differing ionic cavity volumes to below, this comparison considers the same Stern layer parameter $d_{\alpha_{\text{ion}}}$ and fixed smoothness parameters $\xi_{\alpha_{\text{ion}}}^{\pm} = 0.5$ for both cations and anions. For two very different sets of values of $d_{\alpha_{\text{ion}}}$ and the ionic size parameter a , excellent agreement is achieved across a wide range of ionic concentrations. Only for the highly polar cytosine and thin Stern layers, minor deviations can be discerned at the highest ionic concentrations shown. In this regime, ions accumulate significantly in regions of higher electrostatic potential, and the approximations behind the approximate analytical expressions start to break down.

Having validated the approximate analytical expressions, we can proceed with analyzing what this indicates in terms of the SMPB parameter space. For the class of neutral molecules,

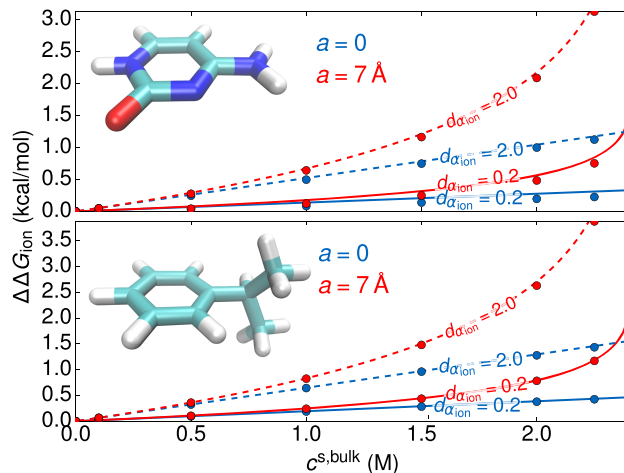


FIG. 2. Calculated $\Delta\Delta G_{\text{ion}}$ as a function of ionic bulk concentration $c^{\text{s,bulk}}$ for the highly polar molecule cytosine (upper panel) and the apolar molecule isopropylbenzene (lower panel). Compared are the results from full SMPB-DFT calculations (filled circles) with the analytical expressions for the Setschenow coefficient of Eq. (12) (red lines) and Eq. (13) (blue lines). Shown are the results for two different ionic sizes a (red vs. blue data) and Stern layer thicknesses $d_{\alpha_{\text{ion}}}$ (dashed vs. solid lines). Equal Stern layer thickness for cations and anions is employed, as well as a fixed $\xi_{\alpha_{\text{ion}}}^{\pm} = 0.5$. In the case $a = 7 \text{ \AA}$, the ionic bulk concentration $c^{\text{s,bulk}} = 2.42 \text{ M}$ represents the upper bound for the physically realistic region in which the lattice occupation of the MPB model by ions $\phi_0 < 1$.

the use of any finite ion size parameter a will intrinsically lead to deviations from the linear Setschenow regime, in particular, at higher ionic concentrations. The actual value of the Setschenow coefficient is instead primarily governed through the choice of the Stern layer thickness, $d_{\alpha_{\text{ion}}}^{\pm}$, and the smoothness of the ionic transition, $\xi_{\alpha_{\text{ion}}}^{\pm}$, as these are the central parameters changing the ionic cavity volumes for a given solute. As apparent from Fig. 2, the choice of a larger ion size parameter can in principle also lead to an increasing slope of $\Delta\Delta G_{\text{ion}}$ in a pseudo-linear regime at lower ionic concentrations and could therefore also be used to effectively fit the experimental values for $\Delta\Delta G_{\text{ion}}$ at a particular concentration. This highlights the afore discussed correlations in the SMPB parameter space. On the basis of the obtained analytical understanding, we expect a low transferability of corresponding $a \neq 0$ parameter sets though. For the targeted class of neutral solutes at low to medium ion concentrations, we instead set $a = 0$ from now on. MPB-like modifications with finite a are instead presumably useful to describe deviations from the Setschenow law at high ion concentrations or in regions of high local ion concentrations as expected for large ion sizes or charged solutes.

To further analyze the role of the remaining four ionic parameters, we compute the Setschenow coefficients for the whole database I with the approximate Eq. (14) for varying choices of $d_{\alpha_{\text{ion}}}^{\pm}$ and $\xi_{\alpha_{\text{ion}}}^{\pm}$. These calculations are done for an ionic bulk concentration of $c^{\text{s,bulk}} = 1 \text{ M}$, at which the Setschenow law is known to hold for most monovalent salt solutions. Evaluating the root mean-square error (RMSE) of the thus estimated Setschenow coefficients for each set of SMPB parameter values with respect to the experimental data clearly demonstrates the expected effect of the total ionic cavity volume as the central feature governing the accuracy

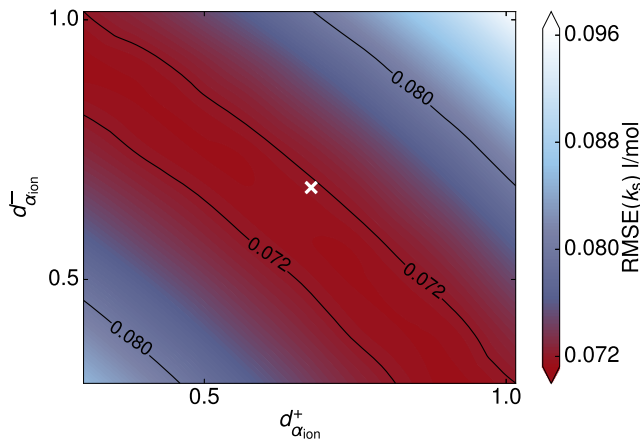


FIG. 3. Root mean-square error (RMSE) for the NaCl training set (database **I**) between calculated (through Eq. (14)) and measured Setschenow coefficients as obtained for different choices of Stern layer parameters $d_{\alpha_{ion}^+}$ and $d_{\alpha_{ion}^-}$ ($a=0$, $\xi_{\alpha_{ion}^\pm} = 0.5$). The optimum RMSE of the full SMPB-DFT approach, achieved for $d_{\alpha_{ion}^+} = d_{\alpha_{ion}^-} = 0.68$, is indicated by a white cross.

of the fit. Parameter combinations that effectively lead to the same total volume ($V_{ion,cav}^+ + V_{ion,cav}^-$) generally achieve the same RMSE. As exemplified by Fig. 3, a larger cationic volume through the choice of a larger cationic Stern layer thickness $d_{\alpha_{ion}^+}$ can for instance be compensated by a smaller anionic volume through the choice of a smaller Stern layer thickness $d_{\alpha_{ion}^-}$ to yield the same RMSE fit. For the given functional form of the transition function for the ionic cavity, Eq. (6), changes of the smoothness parameters $\xi_{\alpha_{ion}^\pm}$ lead to (albeit small) variations of the enclosed volume. Correspondingly, we also obtain a weak sensitivity of the RMSE to the choice of this parameter, where effective increases of the volume through $\xi_{\alpha_{ion}^\pm}$ can again be compensated by reductions of the Stern layer thickness (cf. Fig. S2 in the [supplementary material](#)).

In this situation, unconstrained fitting of all four parameters makes no sense and should rather be guided by physical reasoning. For the targeted alkali-halide electrolytes and their roughly similar cationic and anionic sizes, we therefore employ identical Stern layer thicknesses $d_{\alpha_{ion}^\pm} = d_{\alpha_{ion}}$ and shapes $\xi_{\alpha_{ion}^\pm} = \xi_{\alpha_{ion}}$ for both ion types. Since the Stern layer shape has a similar but weaker impact on the total ionic cavity volume than the thickness parameter, we simply fix it to a value $\xi_{\alpha_{ion}} = 0.5$ that yields a reasonable agreement with the molecular dynamics (MD) data shown in Fig. 4 below. In total, this thus leaves only the Stern layer thickness as a meaningful SMPB parameter to be optimized by fitting to the experimental database.

B. Optimized SMPB model: Strengths and limitations

Under the constraint of equal Stern layer thicknesses for cations and anions, an optimum RMSE of 0.068 l/mol to the experimental Setschenow coefficients of database **I** is achieved for $d_{\alpha_{ion}} = 0.68$, cf. Fig. 3. At a bulk ion concentration of 1 M, this corresponds to an excellent prediction of the solvation free energy change on average to within ~ 0.1 kcal/mol. A good transferability of the thus determined SMPB parameter set is thereby indicated by essentially the same RMSE for the validation database **I_{val}** (see Table **I**). We attribute this predictive power to successfully capturing the correct physics of the

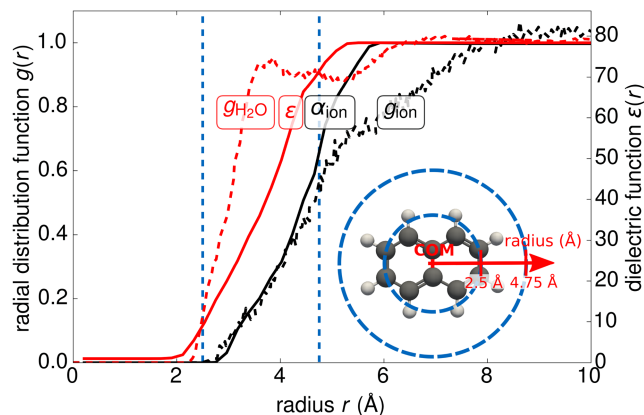


FIG. 4. Comparison of the solvation environment around the center of mass (COM) of naphthalene in a 2.18M NaCl solution. Shown are the spherically-averaged radial distribution functions (RDFs) of the oxygen atoms in the water solvent (g_{H_2O} , dashed red line) and of the sum of both ion types (g_{ion} , dashed black line) as reported by Li *et al.* from all-atom molecular dynamics simulations,⁴⁹ as well as the corresponding spherically-averaged dielectric function $\epsilon(r)$ (solid red line) and ion-exclusion function $\alpha_{ion}(r)$ (solid black line) as obtained with the optimized SMPB model. Both the onset of the solute solvation shell and the radial Stern layer shift of the ionic distribution are rather well reproduced. To better grasp the involved scales, two dotted vertical lines illustrate the radial distance to the molecule COM as shown in the top view in the inset.

ion-specific effects with the established SMPB ion distribution model. This is for instance indicated by comparison to the explicit solute-solvent and solute-ion RDFs obtained from all-atom MD simulations for naphthalene in NaCl solutions by Li *et al.*⁴⁹ As shown in Fig. 4, the onset of the solute solvation shell and the outward Stern layer shift of the ion distribution as modeled by the n_{el} and α_{ion} functions of the optimized SMPB model agree to within a physically reasonable window. As an aside, we found this onset to also be independent of the dielectric function parameterization (cf. Fig. S6 of the [supplementary material](#)) as expected from the validity of Eqs. (13) and (14), additionally supporting the generality of the drawn conclusions about the role of the SMPB parameters.

Interestingly, the RMSE achieved with the effective one-parameter SMPB model is only slightly worse than the one achieved with state-of-the-art multi-parameter data regression

TABLE I. Comparison of the achieved accuracy of the present optimized SMPB model in reproducing experimental Setschenow coefficient databases against models from the literature. This comprises both physically motivated models (TIP3P/TI,⁴⁹ SEA⁴⁹) and descriptor-based approaches (all others^{85,86,108–110}). Stated is the number of parameters involved in the model (#params), the sizes of the training and validation set, and the achieved RMSE (in l/mol) in both sets.

Descriptor/method	#pa-rams	Training		Validation	
		Size	RMSE	Size	RMSE
SMPB	1	95	0.068	33	0.064
pp-LFER ⁸⁵	5	43	0.030	91	0.047
QSPR ¹⁰⁸	4	71	0.030	30	0.043
QSPR (SVM) ¹⁰⁹	4	51	0.019	50	0.029
Connect. inx ¹¹⁰	3	71	0.041	30	0.038
TIP3P/TI ⁴⁹	43	0.084
SEA ⁴⁹	43	0.050

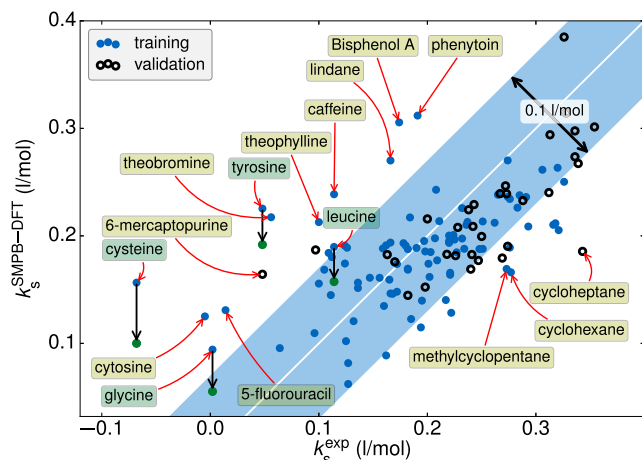


FIG. 5. Comparison of Setschenow coefficients obtained by the optimized SMPB model with the experimental references from the training database **I** (filled circles) and the validation database \mathbf{I}_{val} (empty circles). The light blue region around the correlation line marks an error within 0.05 l/mol. The largest outliers are explicitly labeled with the solute name. Amino acid solutes are marked by darker label color. The black arrows visualize the shift of the calculated Setschenow coefficients for four amino acids when considering a zwitterionic molecular structure, see text.

models, cf. Table I. The main contribution to this RMSE in the training **I** and validation \mathbf{I}_{val} database arises thereby from a small number of highly functionalized and polar molecules, for which the SMPB model strongly overestimates the Setschenow coefficients. These outliers are illustrated in Fig. 5. A similar overestimation for polar molecules has also been reported for regression-model studies,⁸⁵ which points towards experimental uncertainties or an incorrect account of experimental conditions in the models as a reason for the discrepancies. An important aspect to this end could be the actual protonation state of the solute in the measurements, as reference values for k_s are often obtained by averaging over solubility measurements at different pH values.¹¹¹ Since stabilizing electrostatic solute-ion interactions drastically increase for charged molecules, deviations in the protonation state can have a large impact on the determined Setschenow coefficient. In this respect, it is intriguing to realize that amino acids are a prominent group among the outliers in Fig. 5. Close to their isoelectric point, amino acids adopt a zwitterionic form, rather than the neutral geometry which we considered in the calculations by default. Recalculating the SMPB Setschenow coefficients for four such amino acids in the zwitterionic geometry indeed leads to much reduced k_s values in much better agreement with the experimental reference data, cf. Fig. 5.

While this underscores the importance of accurate experimental reference data obtained in carefully adjusted physical conditions, it is nevertheless clear that the SMPB model generally performs worse with increasing polarity of the solute. In fact, when taking the solvation free energy $\Delta G_{\text{sol}}(c^{\text{s,bulk}} = 0)$ as a measure for this polarity, a good correlation can actually be obtained with the signed error in the Setschenow coefficient ($k_s^{\text{SMPB-DFT}} - k_s^{\text{exp}}$) (cf. Fig. S3, in the [supplementary material](#)). This indicates that the SMPB model fails to capture the interactions which are particularly strong for highly polar molecules. This could comprise ion complexation, a reduction of the dielectric permittivity by strong ion-polar group

interactions (dielectric decrement^{112–114}), or solute-ion dispersive interactions, all of which would increase the attractive solute-ion interactions and therewith yield lower k_s values than the ones presently calculated.

More insight can be obtained by considering the vacuum isotropic and static dipole polarizability as obtained from the trace of the diagonalized polarizability tensor $\alpha_0^{\text{iso}} = \text{tr}(\alpha_0)/3$ calculated with density-functional perturbation theory in FHI-aims.¹¹⁵ As put forward by Ninham, Parsons, and Boström, solute-ion dispersion interactions which scale with the solute's polarizability are suspected to play an important role in the explanation of ion-specific effects.^{60,72–76} While, however, the polarizability correlates well with the modeled Setschenow coefficients $k_s^{\text{SMPB-DFT}}$, we found experimental values to be largely independent of it (cf. Figs. S4 and S5, in the [supplementary material](#)). At first sight, the introduction of such artificial correlation could indicate that the electron density representation of the solute volume employed in the present SMPB model might not be optimal to introduce volume correlations in the Setschenow coefficient, at least not throughout the whole database **I**. The good transferability of our SMPB model, however, renders it more plausible that the found correlation would eventually be compensated by the inclusion of so far neglected physical interactions. Among such possible interactions, we do not expect solute-ion dispersion interactions to play a major role, as reasoned from the missing correlation of the experimental data with the dipole polarizabilities. However, in the end, this can only be decided through the development of more advanced PB methods in order to gain more insight into the complex physics of solute-ion interactions.

C. Parameter sets for other monovalent salt solutions

In principle, the SMPB parametrization strategy developed for NaCl solutions can straightforwardly be extended to other monovalent salt solutions. For each salt, an optimized Stern layer thickness is determined by fitting to the experimental Setschenow coefficients of this salt contained in database **II**. Table II summarizes the thus optimized $\alpha_{\text{ion}}^{\text{opt}}$ values. The RMSEs also reported in Table II and the correlation plot in Fig. 6 generally indicate a similar capability and limitations to reproduce the experimental reference data as found for NaCl before. Somewhat higher RMSEs are only obtained for the iodides. We attribute this to strongly attractive solute-ion interactions beyond the reach of the SMPB model. For corresponding molecules like lindane or γ -butyrolactone, these forces lead even to an overall *salting-in* effect, i.e., negative experimental Setschenow coefficients, which the current SMPB model is unable to reproduce.

Unfortunately, the transferability of the thus optimized Stern layer parameters for the other salts is also not as clear as it was the case for the NaCl solution. The corresponding experimental data sets are generally smaller than database **I**, for some salts like LiBr, NaF, NaI, or KF even considerably smaller, cf. Table II. At this scarcity, it is not possible to ensure a balanced and broad range of different organic functionalities in the data set, as was done in database **I** for NaCl. Every reliable empirical Setschenow coefficient is needed for the training; no validation databases can be spared. To nevertheless arrive

TABLE II. Optimized Stern layer parameters $d_{\alpha_{\text{ion}}}^{\text{opt}}$ for monovalent salt solutions. Listed is for each salt the size of the employed training set of experimental Setschenow coefficients as well as the achieved RMSE (in l/mol) over the training set. Detailed lists of the various training sets (database II) are provided in Table S3 in the [supplementary material](#). Data marked with an asterisk could not be completely converged, as the implemented SMPB solver exhibits numerical instabilities at $d_{\alpha_{\text{ion}}} \lesssim 0.09$.

Salt	Size	$d_{\alpha_{\text{ion}}}^{\text{opt}}$	RMSE
LiCl	30	0.46	0.047
LiBr	8	0.27	0.021
NaF	7	1.51	0.026
NaCl	95	0.68	0.068
NaBr	21	0.34	0.064
NaI	6	0.07*	0.127*
KF	9	1.34	0.080
KCl	48	0.48	0.063
KBr	29	0.09*	0.071*
KI	14	0.09*	0.136*
NH ₄ Cl	11	0.13	0.047
NaNO ₃	12	0.08*	0.076*

at some form of independent validation we recall the physical picture behind different Stern layer parameters for the different salts in the SMPB model. As apparent from Fig. 1, corresponding variations would be attributed to different sizes of the hydrated salt ions. As such, one would expect the optimized Stern layer thicknesses for the different salts to roughly scale with empirical hydrated ion sizes.

Static observables like mean ion-water nuclear distances^{117,118} provide thereby only an inappropriate representation of the Stern layer thickness though, as they do not include information about the bonding strength of the hydration shells. Consistent with this expectation, we indeed do not find a correlation of the Stern layer parameters with reported such quantities. A more helpful set of descriptors are

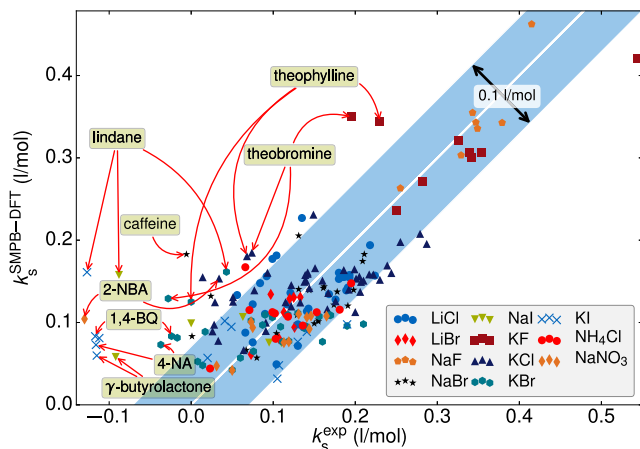


FIG. 6. Correlation of SMPB-DFT calculated Setschenow coefficients with the experimental references of database II. For each salt, the optimized Stern layer thickness parameter $d_{\alpha_{\text{ion}}}^{\text{opt}}$ from Table II is used. The light blue region around the correlation line marks an error within 0.05 l/mol. Some of the points with largest deviations have been exemplarily labeled using the following abbreviations: 1,4-BQ = 1,4-benzoquinone, 4-NA = 4-nitroaniline, 2-NBA = 2-nitrobenzaldehyde.

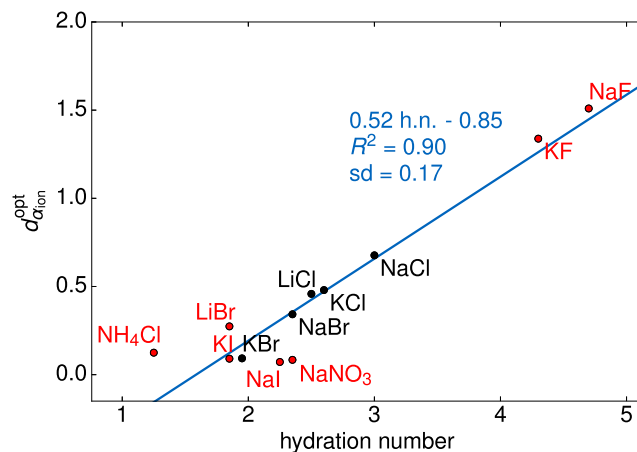


FIG. 7. Correlation of the optimized Stern layer thicknesses $d_{\alpha_{\text{ion}}}^{\text{opt}}$ for different monovalent salts, cf. Table II, with the hydration number as obtained from compressibility data of the bulk electrolyte.¹¹⁶ The linear regression showed a low standard deviation (sd)=0.17 and a high coefficient of determination $R^2=0.90$. The Stern layer parameters marked in red were obtained with training sets containing less than 20 molecules.

instead dynamic hydration sizes which resemble the average sizes of hydrated ions as they propagate through the solution.⁴⁷ These sizes are directly related to the number of strongly bound water molecules (*hydration numbers*) which can be obtained by different experimental techniques.⁷¹ Figure 7 shows that the optimized Stern layer parameters indeed correlate well with such hydration numbers as obtained from compressibility measurements at the infinite dilution limit.¹¹⁶ We thereby averaged the available empirical cation and anion hydration numbers¹¹⁶ to be consistent with the SMPB model using identical Stern layer thicknesses for both ion types. This correlation clearly increases the confidence in the Stern layer parameters given in Table II. This in particular, when considering that the Stern layer parameters with the largest deviations from the regression line were actually also obtained with the smallest training set sizes and that on the contrary the NaCl value as obtained from a converged training set is found directly on top of the line.

The found scaling relation reveals that ion-specific effects on molecular systems can indeed be explained by varying Stern layer thicknesses, which by themselves are determined by the dynamic hydration state of the ions. Moreover, the found correlation between the optimized Stern layer parameters and the hydration numbers can be also used to predict the parameters for other monovalent salts for which experimental Setschenow data are similarly scarce or even scarcer than for the here considered salts. Using the obtained regression expression

$$d_{\alpha_{\text{ion}}}^{\text{opt}} = 0.52 \text{ h.n.} - 0.85, \quad (15)$$

with h.n. the hydration number, to derive the Stern layer thickness parameter, we expect that salt effects can be predicted to a good degree of accuracy for most molecules and monovalent salts. Overall we thus arrive at a rather optimistic perspective on the obtained optimized SMPB models, which suggests their tentative use for production first-principles electrolytic solvation calculations. Notwithstanding, more reliable reference Setschenow coefficients from the experiment would clearly be desirable to fully validate the parameter transferability.

IV. SUMMARY

Stern-layer corrected finite-size modified Poisson-Boltzmann models refine the original Gouy-Chapman solvation theory to account for both the presence of solvated ion-ion (volume-based ion exclusion) and solute-ion (distance-based ion exclusion) repulsive interactions. This comes at the prize of a range of effective ionic parameters that need to be determined. For the use of a SMPB model to describe an electrolytic environment in first-principles electronic structure calculations of solute molecules, optimum such parameters provide maximum transferability, i.e., they allow to reliably treat a wide range of solutes and ion concentrations.

The objective of the present work was to determine corresponding parameters for the much studied class of neutral solutes in aqueous monovalent electrolytes. In corresponding systems, solvation free energy changes with ionic strengths generally show a linear, so-called Setschenow regime up to medium ion concentrations. This suggests to base an empirical SMPB parametrization protocol on reference Setschenow (proportionality) coefficients, which are rather widely available at good accuracy, at least in comparison to other observables sensitive to ion-specific effects. In its full generality, the SMPB implementation in the DFT package FHI-aims comprises five ionic parameters ($a, d_{\alpha_{\text{ion}}}^+, d_{\alpha_{\text{ion}}}^-, \xi_{\alpha_{\text{ion}}}^+, \xi_{\alpha_{\text{ion}}}^-$). They describe the effective size of solvated ions in the MPB lattice model, as well as the extension and shape of the Stern layer for cations and anions with the latter parameters defined in terms of the solute's electron density. As is clear from their physical origin, these parameters are in parts highly correlated, which excludes any unconstrained simultaneous optimization when aiming for transferable parameter sets.

Deriving an approximate analytical expression for the solvation free energy change with ionic strength we could show that for the targeted class of neutral solutes and monovalent electrolytes, the majority of the parameters can be fixed in a salt-independent way. Specifically, we arrive at $a=0$, $\xi_{\alpha_{\text{ion}}}^{\pm}=0.5$ and an equal Stern layer extension for cations and anions $d_{\alpha_{\text{ion}}}^+ = d_{\alpha_{\text{ion}}}^-$. The remaining thickness parameter $d_{\alpha_{\text{ion}}}$ is then optimized for each salt by fitting to a database of empirical Setschenow coefficients from the literature, while an additional dependence of the Stern layer extension on the actual solute molecule is automatically achieved through the dependence of the ion exclusion function on the solute electron density.

For NaCl salt solutions, a high availability of reference Setschenow coefficients allows to determine and validate a highly transferable $d_{\alpha_{\text{ion}}}$. The thus optimized single-parameter SMPB model reproduces measured Setschenow coefficients with an accuracy that is comparable to the prevalent quantitative multilinear regression models and yields solute-ion radial distribution functions that are consistent with the atomically resolved simulation data. Increasing deviations for highly polar molecules thereby point towards the necessity for future SMPB model modifications like a dielectric decrement or solute-ion dispersion interaction corrections.

For monovalent salts other than NaCl, the availability of accurate reference Setschenow coefficients is much lower. Following the established protocol, we could still determine

the optimized Stern layer thickness parameters. However, their transferability could not be fully validated in the same way as for NaCl. On the other hand, we could show that the corresponding $d_{\alpha_{\text{ion}}}$ over the treated range of monovalent electrolytes follow a trend as expected from the empirical ionic hydration numbers, which in turn are directly related to the dynamic ion sizes. This correlation suggests that ion-specific effects for neutral molecules can be straightforwardly explained by varying Stern layer thicknesses which by itself are explainable by different dynamic ion sizes. Moreover, the correlation allows to also evaluate reliable Stern layer parameters for any monovalent salt, i.e., also for the salts for which experimental Setschenow coefficients are not available. Cautiously suggest to employ these parameters for a first account of ion-specific effects in first-principles implicit solvation electronic structure calculations for the corresponding salt solutions. Eventually, we hope this work to trigger new and systematic experimental Setschenow coefficient measurements though, which can then serve as a reliable basis for a future reparametrization following the here established protocol.

SUPPLEMENTARY MATERIAL

See [supplementary material](#) for derivations of the SMPB free energy expression in the case of two different ion exclusion functions and the approximation to the Setschenow coefficient in the case of neutral solutes. Beside that all Setschenow coefficient databases that were used are explicitly listed and the distribution of absolute dipole moments, hydration energies and isotropic, static dipole polarizabilities over the NaCl databases is visualized. Remaining figures show the impact of the Stern layer smoothness and thickness parameter on the quality of the SMPB model, correlations of Setschenow coefficient and signed errors with hydration energy and polarizability, and the dependence of the Stern layer optimized ionic radial distribution function for naphthalene on the choice of the dielectric function.

ACKNOWLEDGMENTS

The authors gratefully acknowledge support from the Solar Technologies Go Hybrid initiative of the State of Bavaria and the German Science Foundation DFG (Grant No. RE1509/21-1). We further would like to thank Professor Alexandre Tkatchenko for insightful discussions and Professor Ken Dill and Dr. Christopher Fennell for access to their Setschenow test set geometries (database **I**, data from Ref. 49).

¹J. Tomasi, B. Mennucci, and R. Cammi, *Chem. Rev.* **105**, 2999–3094 (2005).

²J. L. Fattebert and F. J. Gygi, *J. Comput. Chem.* **23**, 662–666 (2002).

³J. L. Fattebert and F. Gygi, *Int. J. Quantum Chem.* **93**, 139–147 (2003).

⁴D. A. Scherlis, J. L. Fattebert, F. Gygi, M. Cococcioni, and N. Marzari, *J. Chem. Phys.* **124**, 074103 (2006).

⁵O. Andreussi, I. Dabo, and N. Marzari, *J. Chem. Phys.* **136**, 064102 (2012).

⁶C. P. Kelly, C. J. Cramer, and D. G. Truhlar, *J. Chem. Theory Comput.* **1**, 1133–1152 (2005).

⁷S. Ringe, H. Oberhofer, C. Hille, S. Matera, and K. Reuter, *J. Chem. Theory Comput.* **12**, 4052–4066 (2016).

⁸R. Jinnouchi and A. B. Anderson, *Phys. Rev. B* **77**, 245417 (2008).

⁹G. Fisicaro, L. Genovese, O. Andreussi, N. Marzari, and S. Goedecker, *J. Chem. Phys.* **144**, 014103 (2016).

¹⁰K. Mathew and R. G. Hennig, e-print [arXiv:1601.03346](#) (accessed 19 December 2016).

- ¹¹G. Gouy, *J. Phys. Theor. Appl.* **9**, 457–468 (1910).
- ¹²G. Gouy, *Ann. Phys. (Paris)* **7**, 129–184 (1917).
- ¹³D. Chapman, *Philos. Mag.* **25**, 475–481 (1913).
- ¹⁴P. Debye and E. Hückel, *Phys. Z.* **24**, 305–325 (1923).
- ¹⁵S. W. W. Chen and B. Honig, *J. Phys. Chem. B* **101**, 9113–9118 (1997).
- ¹⁶P. Weetman, S. Goldman, and C. G. Gray, *J. Phys. Chem. B* **101**, 6073–6078 (1997).
- ¹⁷F. Fogolari, A. Brigo, and H. Molinari, *J. Mol. Recognit.* **15**, 377–392 (2002).
- ¹⁸R. J. Hunter, *Foundations of Colloid Science* (Oxford University Press, Oxford, 2001), pp. 304–402.
- ¹⁹J. Lipfert, V. B. Chu, Y. Bai, D. Herschlag, and S. Doniach, *J. Appl. Crystallogr.* **40**, s229–s234 (2007).
- ²⁰E. J. W. Verwey and J. T. G. Overbeek, *Theory of the Stability of Lyophobic Colloids* (Elsevier, Amsterdam, 1948).
- ²¹S. Alexander, P. M. Chaikin, P. Grant, G. J. Morales, P. Pincus, and D. Hone, *J. Chem. Phys.* **80**, 5776–5781 (1984).
- ²²J. L. Barrat and J. F. Joanny, *Adv. Chem. Phys.* **94**, 1–66 (1996).
- ²³J. Lyklema, *Fundamentals of Interface and Colloid Science, Volume II: Solid-Liquid Interfaces* (Academic Press, San Diego, 1995), pp. 3.2–4.11.
- ²⁴D. Harries, S. May, W. M. Gelbart, and A. Ben-Shaul, *Biophys. J.* **75**, 159–173 (1998).
- ²⁵I. Borukhov, D. Andelman, and H. Orland, *Macromolecules* **31**, 1665–1671 (1998).
- ²⁶D. Andelman, in *Structure and Dynamics of Membranes: From Cells to Vesicles*, Handbook of Biological Physics, edited by R. Lipowsky and E. S. Sackmann (North-Holland, 1995), Vol. 1, Chap. 12, pp. 603–642.
- ²⁷K. Letchworth-Weaver and T. A. Arias, *Phys. Rev. B* **86**, 075140 (2012).
- ²⁸D. J. Tannor, B. Marten, R. Murphy, R. A. Friesner, D. Sitkoff, A. Nicholls, M. Ringnalda, W. A. Goddard, and B. Honig, *J. Am. Chem. Soc.* **116**, 11875–11882 (1994).
- ²⁹Y.-H. Fang, G.-F. Wei, and Z.-P. Liu, *Catal. Today* **202**, 98–104 (2013).
- ³⁰M. Otani and O. Sugino, *Phys. Rev. B* **73**, 115407 (2006).
- ³¹K. Chin, K. A. Sharp, B. Honig, and A. M. Pyle, *Nat. Struct. Mol. Biol.* **6**, 1055–1061 (1999).
- ³²V. B. Chu, Y. Bai, J. Lipfert, D. Herschlag, and S. Doniach, *Biophys. J.* **93**, 3202–3209 (2007).
- ³³N. Wang, S. Zhou, P. M. Kekenus-Huskey, B. Li, and J. A. McCammon, *J. Phys. Chem. B* **118**, 14827–14832 (2014).
- ³⁴N. A. Baker, D. Sept, S. Joseph, M. J. Holst, and J. A. P. McCammon, *Proc. Natl. Acad. Sci. U. S. A.* **98**, 10037–10041 (2001).
- ³⁵M. K. Gilson, K. A. Sharp, and B. H. Honig, *J. Comput. Chem.* **9**, 327–335 (1988).
- ³⁶I. Borukhov, D. Andelman, and H. Orland, *Electrochim. Acta* **46**, 221–229 (2000).
- ³⁷I. Borukhov, D. Andelman, and H. Orland, *Phys. Rev. Lett.* **79**, 435–438 (1997).
- ³⁸A. H. Boschsitsch and P. V. Danilov, *J. Comput. Chem.* **33**, 1152–1164 (2012).
- ³⁹J. H. Chaudhry, S. D. Bond, and L. N. Olson, *J. Sci. Comput.* **47**, 347–364 (2011).
- ⁴⁰V. Kralj-Iglic and A. Iglic, *J. Phys. II* **6**, 477–491 (1996).
- ⁴¹S. Zhou, Z. Wang, and B. Li, *Phys. Rev. E* **84**, 021901 (2011).
- ⁴²A. Abrashkin, D. Andelman, and H. Orland, *Phys. Rev. Lett.* **99**, 077801 (2007).
- ⁴³G. Tresset, *Phys. Rev. E* **78**, 061506 (2008).
- ⁴⁴A. R. Silalahi, A. H. Boschsitsch, R. C. Harris, and M. O. Fenley, *J. Chem. Theory Comput.* **6**, 3631–3639 (2010).
- ⁴⁵G. J. Bartlett, C. T. Porter, N. Borkakoti, and J. M. Thornton, *J. Mol. Biol.* **324**, 105–121 (2002).
- ⁴⁶O. Stern, *Z. Elektrochem. Angew.* **30**, 508–516 (1924).
- ⁴⁷M. Y. Kiriukhin and K. D. Collins, *Biophys. Chem.* **99**, 155–168 (2002).
- ⁴⁸M. A. Brown, A. Goel, and Z. Abbas, *Angew. Chem., Int. Ed.* **55**, 3790–3794 (2016).
- ⁴⁹L. Li, C. J. Fennell, and K. A. Dill, *J. Chem. Phys.* **141**, 22D518 (2014).
- ⁵⁰B. Honig and A. Nicholls, *Science* **268**, 1144–1149 (1995).
- ⁵¹Y.-H. Fang and Z.-P. Liu, *J. Am. Chem. Soc.* **132**, 18214–18222 (2010).
- ⁵²H.-F. Wang and Z.-P. Liu, *J. Phys. Chem. C* **113**, 17502–17508 (2009).
- ⁵³R. Jinnouchi, K. Kodama, T. Hatanaka, and Y. Morimoto, *Phys. Chem. Chem. Phys.* **13**, 21070–21083 (2011).
- ⁵⁴D. Boda, W. R. Fawcett, D. Henderson, and S. Sokolowski, *J. Chem. Phys.* **116**, 7170–7176 (2002).
- ⁵⁵K. Bohinc, A. Shrestha, M. Brumen, and S. May, *Phys. Rev. E* **85**, 031130 (2012).
- ⁵⁶Y. X. Yu, J. Z. Wu, and G. H. Gao, *J. Chem. Phys.* **120**, 7223–7233 (2004).
- ⁵⁷J. Cervera, P. Ramirez, J. A. Manzanares, and S. Mafe, *Microfluid. Nanofluid.* **9**, 41–53 (2010).
- ⁵⁸M. S. Kilic, M. Z. Bazant, and A. Ajdari, *Phys. Rev. E* **75**, 021503 (2007).
- ⁵⁹D. Antypov, M. C. Barbosa, and C. Holm, *Phys. Rev. E* **71**, 061106 (2005).
- ⁶⁰M. Boström, F. W. Tavares, D. Bratko, and B. W. Ninham, *J. Phys. Chem. B* **109**, 24489–24494 (2005).
- ⁶¹M. O. Fenley, R. C. Harris, B. Jayaram, and A. H. Boschsitsch, *Biophys. J.* **99**, 879–886 (2010).
- ⁶²S. Kirmizialtin, A. R. Silalahi, R. Elber, and M. O. Fenley, *Biophys. J.* **102**, 829–838 (2012).
- ⁶³R. C. Harris, A. H. Boschsitsch, and M. O. Fenley, *J. Chem. Phys.* **140**, 075102 (2014).
- ⁶⁴I. Sechenow, *Ann. Chim. Phys.* **25**, 226 (1892).
- ⁶⁵F. Long and W. McDevitt, *Chem. Rev.* **51**, 119–169 (1952).
- ⁶⁶V. Blum, R. Gehrke, F. Hanke, P. Havu, V. Havu, X. Ren, K. Reuter, and M. Scheffler, *Comput. Phys. Commun.* **180**, 2175–2196 (2009).
- ⁶⁷X. Ren, P. Rinke, V. Blum, J. Wierferink, A. Tkatchenko, A. Sanfilippo, K. Reuter, and M. Scheffler, *New J. Phys.* **14**, 053020 (2012).
- ⁶⁸V. L. Shapovalov and G. J. Brezesinski, *Phys. Chem. B* **110**, 10032–10040 (2006).
- ⁶⁹B. Jayaram, S. Swaminathan, D. Beveridge, K. Sharp, and B. Honig, *Macromolecules* **23**, 3156–3165 (1990).
- ⁷⁰D. J. Bonthuis and R. R. Netz, *J. Phys. Chem. B* **117**, 11397–11413 (2013).
- ⁷¹Y. Marcus, *Ions in Solution and their Solvation* (Wiley, New Jersey, USA, 2015), pp. 141–146.
- ⁷²B. W. Ninham, T. T. Duignan, and D. F. Parsons, *Curr. Opin. Colloid Interface Sci.* **16**, 612–617 (2011).
- ⁷³D. F. Parsons and B. W. Ninham, *Colloids Surf., A* **383**, 2–9 (2011).
- ⁷⁴D. F. Parsons, M. Boström, P. L. Nostro, and B. W. Ninham, *Phys. Chem. Chem. Phys.* **13**, 12352–12367 (2011).
- ⁷⁵M. Boström, D. R. M. Williams, and B. W. Ninham, *Langmuir* **17**, 4475–4478 (2001).
- ⁷⁶M. Boström, D. Williams, and B. W. Ninham, *Biophys. J.* **85**, 686–694 (2003).
- ⁷⁷X. Pang and H.-X. Zhou, *Commun. Comput. Phys.* **13**, 1–12 (2013).
- ⁷⁸F. Dong, M. Vijayakumar, and H.-X. Zhou, *Biophys. J.* **85**, 49–60 (2003).
- ⁷⁹P. Pérez-Tejeda, A. Maestre, M. Balón, J. Hidalgo, M. A. Muñoz, and M. Sánchez, *J. Chem. Soc., Faraday Trans. 1* **83**, 1029–1039 (1987).
- ⁸⁰A. Burant, G. V. Lowry, and A. K. Karamalidis, *Chemosphere* **144**, 2247–2256 (2016).
- ⁸¹D. F. Keeley, M. A. Hoffpauir, and J. R. Meriwether, *J. Chem. Eng. Data* **33**, 87–89 (1988).
- ⁸²E. M. Waxman, J. Elm, T. Kurtén, K. V. Mikkelsen, P. J. Ziemann, and R. Volkamer, *Environ. Sci. Technol.* **49**, 11500–11508 (2015).
- ⁸³P. Debye and I. MacAulay, *Phys. Z.* **131**, 22–29 (1925).
- ⁸⁴W.-H. Xie, W.-Y. Shiu, and D. Mackay, *Mar. Environ. Res.* **44**, 429–444 (1997).
- ⁸⁵S. Endo, A. Pfennigsdorff, and K.-U. Goss, *Environ. Sci. Technol.* **46**, 1496–1503 (2012).
- ⁸⁶N. Ni and S. H. Yalkowsky, *Int. J. Pharm.* **254**, 167–172 (2003).
- ⁸⁷W. Xie, H. Ji, and W. Li, *Acta Phys.-Chim. Sin.* **1**, 304–307 (1985).
- ⁸⁸M. A. Paul, *J. Am. Chem. Soc.* **74**, 5274–5277 (1952).
- ⁸⁹H. Kruyt and C. Robinson, *Proc. Acad. Sci. Amsterdam* **29**, 1244 (1926).
- ⁹⁰R. L. Bergen and F. A. Long, *J. Phys. Chem.* **60**, 1131–1135 (1956).
- ⁹¹A. Osol and M. Kilpatrick, *J. Am. Chem. Soc.* **55**, 4430–4440 (1933).
- ⁹²J. N. Sugden, *J. Chem. Soc.* **129**, 174–196 (1926).
- ⁹³W. Herz and E. Stanner, *Z. Phys. Chem.* **128**, 399 (1927).
- ⁹⁴P. Groß and K. Schwarz, *Monatsh. Chem. Verw. Teile Anderer Wiss.* **55**, 287–306 (1930).
- ⁹⁵W. L. Masterton and T. P. Lee, *Environ. Sci. Technol.* **6**, 919–921 (1972).
- ⁹⁶A. Al-Maaieh and D. R. Flanagan, *J. Pharm. Sci.* **91**, 1000–1008 (2002).
- ⁹⁷F. I. El-Dossoki, *J. Chem.* **2016**, 1–8.
- ⁹⁸M. Randall and C. F. Failey, *Chem. Rev.* **4**, 285–290 (1927).
- ⁹⁹M. Randall and C. F. Failey, *Chem. Rev.* **4**, 271–284 (1927).
- ¹⁰⁰M. Randall and C. F. Failey, *Chem. Rev.* **4**, 291–318 (1927).
- ¹⁰¹A. G. Leiga and J. N. Sarmousakis, *J. Phys. Chem.* **70**, 3544–3549 (1966).
- ¹⁰²J. C. Philip and A. Bramley, *J. Chem. Soc., Trans.* **107**, 377–387 (1915).
- ¹⁰³T. J. Morrison and F. Billett, *J. Chem. Soc.* **1952**, 3819–3822.
- ¹⁰⁴J. P. Perdew, K. Burke, and M. Ernzerhof, *Phys. Rev. Lett.* **77**, 3865–3868 (1996).
- ¹⁰⁵W. E. May, S. P. Wasik, and D. H. Freeman, *Anal. Chem.* **50**, 997–1000 (1978).
- ¹⁰⁶G. Gold and S. Rodriguez, *Can. J. Chemistry* **67**, 822–826 (1989).
- ¹⁰⁷R. R. Netz and H. Orland, *Euro. Phys. J. E* **1**, 203–214 (2000).

- ¹⁰⁸Q. Xu, L. Fan, and J. Xu, *Maced. J. Chem. Chem. Eng.* **35**, 53–62 (2016).
- ¹⁰⁹X. Yu and R. Yu, *Ind. Eng. Chem. Res.* **52**, 11182–11188 (2013).
- ¹¹⁰Y. Li, Q. Hu, and C. Zhong, *Ind. Eng. Chem. Res.* **43**, 4465–4468 (2004).
- ¹¹¹R. Carta and G. Tola, *J. Chem. Eng. Data* **41**, 414–417 (1996).
- ¹¹²A. Levy, D. Andelman, and H. Orland, *Phys. Rev. Lett.* **108**, 227801 (2012).
- ¹¹³H. Li and B. Lu, *J. Chem. Phys.* **141**, 024115 (2014).
- ¹¹⁴Y. Nakayama and D. Andelman, *J. Chem. Phys.* **142**, 044706 (2015).
- ¹¹⁵H. Shang, C. Carbogno, P. Rinke, and M. Scheffler, “Lattice dynamics calculations based on density-functional perturbation theory in real space,” *Comput. Phys. Commun.* (in press).
- ¹¹⁶Y. Marcus, *Ions in Solution and their Solvation* (Wiley, New Jersey, USA, 2015), pp. 145–146.
- ¹¹⁷H. Ohtaki, *Monatsh. Chem.* **132**, 1237–1268 (2001).
- ¹¹⁸Y. Marcus, *Chem. Rev.* **88**, 1475–1498 (1988).